THE ASTROPHYSICAL JOURNAL SUPPLEMENT SERIES, 63:295–310, 1987 February

SPECTRAL CLASSIFICATION OF EMISSION-LINE GALAXIES[1]

SYLVAIN VEILLEUX AND DONALD E. OSTERBROCK
Lick Observatory and Board of Studies in Astronomy and Astrophysics, University of California, Santa Cruz
Received 1986 June 4; accepted 1986 August 12

ABSTRACT

A revised method of classification of narrow-line active galaxies and H II region–like galaxies is proposed. It involves the line ratios [O III] $\lambda 5007/H\beta$, [N II] $\lambda 6583/H\alpha$, [S II] $(\lambda 6716+\lambda 6731)/H\alpha$, and [O I] $\lambda 6300/H\alpha$. These line ratios take full advantage of the physical distinction between the two types of objects and minimize the effects of reddening correction and errors in the flux calibration. Large sets of internally consistent data are used, including new, previously unpublished measurements. Predictions of recent photoionization models by power-law spectra and by hot stars are compared with the observations. The classification is based on the observational data interpreted on the basis of these models.

Subject headings: galaxies: Seyfert

I. INTRODUCTION

An important fraction of galaxies have narrow emission lines in their spectra. Meurs (Meurs 1982; Meurs and Wilson 1984) has shown that at $M_p = -21$ about 10% of all field galaxies are Markarian galaxies, and, of these, about 10% are Seyfert galaxies. By $M_p = -23$ essentially all galaxies are Markarian galaxies, nearly all of which are Seyfert galaxies. Markarian galaxies that are not Seyfert galaxies generally have emission-line spectra similar to those of H II regions (Huchra 1977); evidently these objects contain gas that is photoionized by hot stars, and they are therefore called H II region–like galaxies (French 1980). The most luminous objects of this type with the strongest emission lines are called starburst galaxies (Weedman *et al.* 1981; Balzano 1983).

Seyfert galaxies, the most frequent type of active galactic nuclei (AGNs), have bright, semistellar nuclei, and spectra with broad emission lines covering a wide range of ionization (Khachikian and Weedman 1974). Narrow-emission-line Seyferts or Seyfert galaxies of type 2 are defined by the property that their permitted lines and forbidden lines have similar widths, of the order of 5×10^2 km s^{-1} (Khachikian and Weedman 1974). Their radio-selected counterparts, the narrow-line radio galaxies, have properties very similar to the Seyfert 2 galaxies. Both groups will be included in this study. They both appear to be photoionized by a "nonthermal" or "power-law" continuum (Koski 1978).

Another class of narrow-emission-line AGNs is made up of low-ionization nuclear emission-line regions (LINERs) (Heckman 1980). Their spectra include strong low-ionization lines such as [O I] $\lambda 6300$ and [S II] $\lambda\lambda 6716, 6731$; in this respect they show a wider range of ionization stages than the emission-line spectra produced in H II regions. Identifying the ionization mechanism in LINERs has been the goal of a number of recent investigations (Heckman 1980; Stauffer 1982; Ferland and Netzer 1983; Halpern and Steiner 1983; Keel 1983; Binette 1985; Stasinska 1984*b*). At present it seems most likely that their ionization is due primarily to "power-law" continua similar to those responsible for the emission-line spectra of Seyfert 2 galaxies.

This same ionization mechanism also appears to be dominant in Seyfert 1 galaxies and broad-line radio galaxies, in which the H I lines are significantly broader than the forbidden lines (see, e.g., Osterbrock 1984). Seyfert 1.5, 1.8, and 1.9 galaxies have similarly broad components of the H I lines. We shall exclude all these objects from the remainder of the present paper and confine our attention to Seyfert 2 galaxies, narrow-line radio galaxies, H II region galaxies, and LINERs, all of which we shall lump together as "emission-line galaxies."

Possibly the best way we have to test our understanding of the different mechanisms responsible for the ionization in emission-line galaxies is to consider a large sample of these objects with well-measured spectra, and try to determine which spectral features differentiate objects in which the photoionization is by hot OB stars from objects in which the photoionization is due to a nonthermal or "power-law" continuum. On the basis of a limited sample of emission-line galaxies, Shuder and Osterbrock (1981) found that the criterion [O III] $\lambda 5007/H\beta \gtrsim 3$ was a good basis for defining an object as a Seyfert 2. Since then, however, some starburst galaxies have been found to be sufficiently highly ionized so that this ratio exceeds 3 (Balzano 1983; Osterbrock 1985). Indeed, some of the "galaxies with the spectra of H II regions" studied by French (1980) have [O III] $\lambda 5007/H\beta > 3$. Also, in most LINERs, [O III] $\lambda 5007/H\beta < 3$ (Keel 1983). We know that H II region–like galaxies can be distinguished from Seyfert 2 galaxies by the weakness of low-ionization lines such as [N II] $\lambda 6583$, [S II] $\lambda\lambda 6716, 6731$, and especially [O I] $\lambda 6300$. The [S II] and [O I] emission lines arise preferentially in a zone of partly ionized hydrogen. This zone is quite extended in objects photoionized by a spectrum containing a large fraction of high-energy photons, but is nearly absent in galaxies photoionized by OB stars. This is the physical difference that distinguishes a narrow-line AGN from

[1] *Lick Observatory Bulletin*, No. 1049.

an H II region–like object. It is the basis of the classification scheme of Baldwin, Phillips, and Terlevich (1981, hereafter BPT).

In the present paper we propose a revised method of classification of narrow-line AGNs and H II region–like galaxies that takes full advantage of the physical distinction between the two types of objects. It is based on line ratios involving [O III] λ5007, [N II] λ6583, [S II] λλ6716, 6731, [O I] λ6300, and the Balmer lines. It excludes reddening-sensitive line ratios such as [O II] λ3727/[O III] λ5007 used by BPT. Since that paper appeared, large sets of data on emission-line galaxies have been published by Keel (1983) and Balzano (1983). These and other recent data will be included in our analysis. Our theoretical understanding of emission-line galaxies has also improved considerably during the last five years. Important publications of photoionization models by power-law spectra (Ferland and Netzer 1983; Halpern and Steiner 1983; Binette 1985; Stasinska 1984*a*, *b*) and by hot stars (Stasinska 1980, 1982; Evans and Dopita 1985; McCall, Rybski, and Shields 1985) will be discussed, since they can help discriminate between the two classes of objects.

The plan of this paper is as follows. In § II the choice of line ratios is discussed. Next, the observational material used in this study is described. Then the procedure used to correct for interstellar reddening is discussed. The classification-sensitive line ratios are then plotted in three different diagrams. In § III those diagrams are discussed in the context of photoionization models based on power-law continua and hot stars. In the interest of completeness, shock heating is also investigated. Quantitative criteria for classifying emission-line galaxies are presented and applied in § IV. Finally, in § V, the important results of this work are summarized and the usefulness of the revised classification is briefly discussed.

II. OBSERVATIONS

a) *Choice of Line Ratios*

Before describing the data sample, a few comments on the choice of line intensity ratios on which to base the classification will be useful. It is well known that the emission-line spectra of H II regions can be classified using only one parameter such as {[O II] (λ3726 + λ3729) + [O III] (λ4959 + λ5007)}/Hβ (McCall, Rybski, and Shields 1985). Unfortunately, AGNs cannot be classified with a single parameter. Classification systems based on at least two line intensity ratios are needed.

The search for the best line ratios for two-dimensional classification of emission-line galaxies can be narrowed down by five criteria:

1. Each ratio should be made up of strong lines that are easy to measure in typical spectra.
2. Lines that are badly blended with other lines should be avoided because the somewhat subjective nature of the deblending procedure increases the uncertainty in the flux measurements of these lines.
3. The wavelength separation between the two lines should be as small as possible so that the ratio is relatively insensitive to reddening and flux calibration.

TABLE 1

SOURCES OF PUBLISHED DATA

Reference	Type of Object[a]
Balzano 1983	SBG
Costero and Osterbrock 1977	RG
Dinerstein and Shields 1986	H II
French 1980	H II G
Keel 1983	L
Koski 1978	S2, RG, NELG
McCall, Rybski, and Shields 1985	H II
Shuder and Osterbrock 1981	S2, RG, NELG

[a] S2 = Seyfert 2; RG = narrow-line radio galaxy; L = LINER; SBG = starburst galaxy; H II G = H II region–line galaxy; H II = H II region in external galaxy (including in nucleus); NELG = narrow–emission-line galaxy (either LINER or H II region–like galaxy).

4. Ratios involving a line of only one element and an H I Balmer line should be preferred to those involving forbidden lines of different elements, because they are less abundance-sensitive.
5. The lines should be in a region of the spectrum that is easily accessible with present-day instruments. Among other considerations, lines in the ultraviolet should be avoided because of the low sensitivity of many CCDs at short wavelengths.

The line ratios that satisfy all five criteria are [O III] λ5007/Hβ, [N II] λ6583/Hα (which are proportional to [O III] (λ4959 + λ5007)/Hβ and [N II] (λ6548 + λ6583)/Hα, respectively), and [S II] (λ6716 + λ6731)/Hα. [O II] λ3727/[O III] λ5007, used as an ionization parameter by BPT, is far more sensitive to reddening corrections and calibration errors than [O III] λ5007/Hβ. The problem of deblending Hα from [N II] λλ6548, 6583 is troublesome but not too critical, because spectra of most of the galaxies were taken at sufficiently high resolution to determine the ratio [N II] λ6583/Hα with relatively good accuracy. We also included [O I] λ6300/Hα in our study in spite of the weakness of [O I] in H II region–like objects because, as BPT showed, it is perhaps the best discriminator available between photoionization by "power-law" spectra and by OB stars.

b) *Data Sample*

This study is based on a sample of 264 objects: 105 H II regions in external galaxies, 37 H II region–like galaxies (including 23 starburst galaxies), 41 Seyfert 2 galaxies, 30 LINERs, 10 narrow-line radio galaxies, and 41 other objects that have been called in the past "narrow–emission-line galaxies" (NELGs) because their emission-line ratios [O III] λ5007/Hβ were smaller than those of Seyfert 2 galaxies (Shuder and Osterbrock 1981). They are either LINERs or H II region galaxies.

An important fraction of this sample was compiled from the literature. Table 1 lists the sources used. These papers were selected because they contained large sets of recently obtained and internally consistent data. All the line strengths are based on spectrophotometric measurements taken either

with a SIT Vidicon spectrometer (Balzano 1983) or with an image-tube image-dissector scanner (IDS) system (all the others). The contamination of the emission lines by the underlying stellar population of the galaxy was corrected for using different methods. Costero and Osterbrock (1977), Koski (1978), and Shuder and Osterbrock (1981) all used essentially the same procedure, subtracting from the spectra of the emission-line galaxies the continuum of the nuclear region of a "typical" elliptical (NGC 6482 or NGC 6702) or early-type spiral galaxy (NGC 2681). Since it is uncertain that these spectra are identical with those of the underlying stellar population contribution in the emission-line galaxies, Costero and Osterbrock (1977) and Shuder and Osterbrock (1981) also measured the line fluxes from the original unsubtracted scans and averaged these values with those obtained from the subtracted scans. Keel (1983) used instead a stellar synthesis technique in which the whole spectrum of each galaxy was modeled as a sum of the spectra of various stellar population components. McCall, Rybski, and Shields (1985) used the measured equivalent widths of Hγ and Hβ to determine the equivalent widths of the underlying Balmer absorption. They adopted a constant absorption equivalent width of 1.9 Å for these two Balmer lines to correct all their data. Dinerstein and Shields (1986) used the same method for NGC 4861, but adopted a smaller absorption equivalent width, 1.0 Å, from a detailed discussion of the Balmer gradient in this one galaxy.

The methods used to correct the line fluxes for the effect of intrinsic reddening also differ from one paper to another. In an attempt to obtain an internally consistent sample, we applied, when possible, a single dereddening procedure to all the original data. This point will be discussed in greater detail in § II*d* below.

c) *Additional Measurements*

The line ratios in the spectra of 26 emission-line galaxies from the sample of Osterbrock and Dahari (1983) were measured and included in the present study. They classified 12 of these objects as Seyfert 2 galaxies, and called the remaining objects NELGs. Our measured line ratios for these galaxies are listed in Table 2. For the objects in which the underlying stellar population continuum affected the emission-line spectrum of the galaxy, the template correction procedure of Shuder and Osterbrock (1981) was used. Note that in Table 2 (and subsequently in Tables 3 and 4 also) the logarithms of the ratios are given for [O III] λ5007/Hβ, [N II] λ6583/Hα, [S II] (λ6716 + λ6731)/Hα, [O I] λ6300/Hα, and Hα/Hβ. The values listed for Mrk 266 SW and Mrk 1066 were measured by Osterbrock and Dahari (1983) and Goodrich and Osterbrock (1983), respectively. Note that in these tables the first line for each object lists the measured ratios, while the second line gives the calculated ratios, corrected for interstellar extinction as discussed below.

The spectra of another group of 17 emission-line galaxies, selected as possible Seyfert candidates and observed with the CCD transmission-grism spectrograph (Lauer *et al.* 1984) at the Cassegrain focus of the Shane 3 m telescope, were analyzed and the line ratios measured. The results are presented in Table 3. Measured heliocentric redshifts from these same spectra are also listed. From previous experience with this spectrograph (Osterbrock and De Robertis 1985) the uncertainties in the redshift are typically ±0.0002.

Finally, seven starburst galaxies taken from the sample of Balzano (1983) were observed with an image-tube IDS at the Nickel 1 m telescope or with the CCD transmission grating spectrograph at the Shane 3 m. These results are included in Table 3 (Shane CCD) or are listed in Table 4 (Nickel IDS).

d) *Reddening*

There is no doubt of the presence of dust in Seyfert galaxies and in H II region galaxies, nor that it modifies the spectra of these objects. However, to correct accurately for its extinction is difficult. Since very little is known of the properties of dust in these galaxies, the standard assumption is that the optical properties of the dust in emission-line galaxies are identical with the optical properties of dust in our Galaxy near the Sun. Furthermore, we have only a meager knowledge of the real distribution of dust in emission-line galaxies. It seems quite likely that it is patchy and irregular, and thus that the assignment of a single value for "the extinction" is only a crude first approximation.

Several methods have been developed in order to correct the emission-line spectra for the presence of dust. Perhaps the most widely used is based on the relative strengths of the lower Balmer lines. Usually the observed Balmer-line relative intensities are compared with the calculated values. The observed Balmer decrement is invariably steeper than the calculated decrement. The difference is then assumed to be due to interstellar extinction. The amount of interstellar extinction obtained using this method generally agrees relatively well with the amount of extinction determined using other line ratios such as He II λ3203/He II λ4686 (Shuder and Osterbrock 1981) or [S II] λ4071/[S II] λ10320 (Wampler 1971; Shields and Oke 1975; Koski 1978). A problem with the Balmer-line method is the large uncertainty in the measured strengths of Hγ, Hδ, etc., because of their intrinsic weakness and because they can be strongly affected by the underlying stellar Balmer absorption lines. In order to have an internally consistent sample, we applied this method to each of our objects (except the galaxies of Keel 1983; see below), using only the ratio of the two strongest Balmer lines, Hα/Hβ, to determine the amount of extinction.

The effect of reddening on the ratio Hα/Hβ can be written

$$\frac{I(\mathrm{H}\alpha)}{I(\mathrm{H}\beta)} = \frac{F(\mathrm{H}\alpha)}{F(\mathrm{H}\beta)} 10^{c[f(\mathrm{H}\alpha)-f(\mathrm{H}\beta)]},$$

where c is the measure of the amount of reddening [$E(B-V) = 0.77c$], $f(\lambda)$ is the reddening curve, $I(\lambda)$ is the (unreddened) intrinsic flux, and $F(\lambda)$ is the observed flux. The Whitford reddening curve as parameterized by Miller and Mathews (1972) was used. This means that we have assumed that extinction removes photons from the beam and that scattering of other photons into the beam is negligible. This assumption is correct for stars from which the form of the interstellar reddening curve is determined, but is clearly incorrect for unresolved galactic nuclei and H II regions in which the dust is close to or within the source, and is observed in the slit with the object. However, the assumption may not be too

TABLE 2

MEASURED AND CORRECTED EMISSION-LINE RATIOS FOR SEYFERT GALAXIES AND SEYFERT GALAXY CANDIDATES[a]

Mrk	log [O III]/Hβ	log [N II]/Hα	log [S II]/Hα	log [O I]/Hα	log Hα/Hβ	z,[b] c	Class
266 SW[c,d]	+0.68[a]	−0.21	−0.41	−1.19	0.77	0.0276, 0.85	S2
	+0.65[a]	−0.21	−0.43	−1.16	0.49		
403	+1.08	−0.03	−0.44	−1.11	0.64	0.0244, 0.46	S2
	+1.06	−0.03	−0.45	−1.09	0.49		
533[c]	+1.09	−0.05	−0.52	−1.06	0.65:	0.0289, 0.47:	S2
	+1.07	−0.05	−0.53	−1.04	0.49		
686[c]	+1.02::	+0.17	+0.03	−0.56	0.51::	0.0140, 0.06::	S2
	+1.02::	+0.17	+0.03	−0.55	0.49		
917[c]	+0.79	−0.09	−0.46	−1.08	0.90	0.0242, 1.23	S2
	+0.74	−0.09	−0.49	−1.03	0.49		
955[c]	+0.53:	−0.13	−0.45	−1.22	0.91:	0.0349, 1.27:	S2
	+0.49:	−0.14	−0.48	−1.17	0.49		
1058	+1.06	−0.02	−0.21	−1.09	0.77	0.0169, 0.82	S2
	+1.03	−0.02	−0.22	−1.06	0.49		
1066[c,d]	+0.64	−0.06	−0.38	−1.08	0.89	0.0120, 1.20	S2
	+0.59	−0.06	−0.41	−1.03	0.49		
1073[c]	+0.92	−0.04	−0.42	−1.18	0.80	0.0233, 0.92	S2
	+0.88	−0.04	−0.44	−1.14	0.49		
1157[c]	+1.01	+0.06	−0.21	−0.89	0.67	0.0151, 0.52	S2
	+0.99	+0.05	−0.22	−0.87	0.49		
1457	+1.04	−0.09	−0.52	−1.05	0.96	0.0487, 1.40	S2
	+0.99	−0.10	−0.55	−1.00	0.49		
MCG 05-23-16	−0.40::	−0.11::	−0.06::	−0.29::	0.51::	0.0442, 0.06::	S2
	−0.40::	−0.11::	−0.07::	−0.28::	0.49		
266 NE[c]	+0.10	−0.19	−0.36	−0.92	0.54	0.0277, 0.15	NELG
	+0.10	−0.19	−0.36	−0.91	0.49		
938[c]	> 0.21:	+0.12	−0.40	−1.04	> 0.99:	0.0191, 1.50:	NELG
	> 0.15:	+0.12	−0.43	−0.98	0.49		
945[c]	> 0.45:	−0.06:	−0.13:	...	> 0.14:	0.0152, 0.00:	NELG
	> 0.45:	−0.06:	−0.13:	...	0.49		
1127[c]	> 0.60:	−0.02	−0.29	−0.98	> 0.70:	0.0251, 0.63:	NELG
	> 0.58:	−0.03	0.31	−0.96	0.49		
1133	−0.02	−0.18	−0.40	−1.08	0.80	0.0247, 0.92	NELG
	−0.05	−0.18	−0.42	−1.04	0.49		
1149[c]	−0.37	−0.34	−0.59	−1.56:	0.89	0.0210, 1.30	NELG
	−0.42	−0.34	−0.62	−1.51:	0.45		
1178	−0.19	−0.43	−0.57	−1.44:	0.82	0.0232, 1.08	NELG
	−0.24	−0.44	−0.59	−1.40:	0.45		
1259[c]	+0.23	−0.53	−0.91	−1.79	0.70	0.0070, 0.74	NELG
	+0.20	−0.53	−0.93	−1.77	0.45		
1308[c]	−0.11	−0.60	−0.75	...	0.70	0.0037, 0.74	NELG
	−0.13	−0.60	−0.76	...	0.45		
1344[c]	+0.47	−0.39	−0.47	−1.09	1.01	0.0105, 1.57	NELG
	+0.41	−0.39	−0.50	−1.03	0.49		

TABLE 2—*Continued*

Mrk	$\log \frac{[O\ III]}{H\beta}$	$\log \frac{[N\ II]}{H\alpha}$	$\log \frac{[S\ II]}{H\alpha}$	$\log \frac{[O\ I]}{H\alpha}$	$\log \frac{H\alpha}{H\beta}$	z,[b] c	Class
1459	+0.67	−1.11	−0.78	−1.48	0.76	0.0267, 0.92	NELG
	+0.63	−1.11	−0.80	−1.45	0.45		
1485[c].....	+0.04	−0.09	−0.58	≤ −1.49:	0.83	0.0076, 1.11	NELG
	+0.00	−0.09	−0.61	≤ −1.44:	0.45		
Akn[c] 534	−0.47::	−0.30	−0.65	...	>1.00:	0.0161, 1.55:	NELG
	−0.53::	−0.30	−0.68	...	0.45		
Kaz 27	−0.33	−0.48	−0.62	≤ −1.59:	0.67	0.0412, 0.65	NELG
	−0.35	−0.48	−0.63	≤ −1.56:	0.45		

[a] In cols. (2)–(6) of Tables 2–4 the first line for each object lists the measured ratios, while the second line gives the calculated ratios, corrected for interstellar extinction.

[b] All redshifts are from Osterbrock and Dahari (1983).

[c] Other names: Mrk 266 = NGC 5256, Mrk 533 = NGC 7674, Mrk 686 = NGC 5695, Mrk 917 = MCG 05-53-09, Mrk 938 = NGC 34, Mrk 945 = MCG 01-02-12, Mrk 955 = MCG 00-02-94, Mrk 1066 = MCG 06-07-27, Mrk 1073 = MCG 07-07-37, Mrk 1127 = NGC 7466, Mrk 1149 = MCG 03-03-08, Mrk 1157 = NGC 591, Mrk 1259 = IC 630, Mrk 1308 = IC 745, Mrk 1344 = NGC 4990, Mrk 1485 = NGC 5350, Akn 534 = MCG 06-39-25.

[d] Published data: Mrk 266 SW: Osterbrock and Dahari 1983; Mrk 1066: Goodrich and Osterbrock 1983.

critical, since Mathis (1970) has shown that the *relative* line fluxes calculated allowing for scattering and absorption are not significantly different from those calculated by the standard method. Basically, this is due to the fact that extinction (absorption and scattering) varies smoothly with wavelength and that the standard procedure forces the results to be correct at Hβ and Hα.

For the intrinsic flux ratio for H II region–like objects we adopted the case B Balmer recombination decrement $I(H\alpha)/I(H\beta) = 2.85$ for $T = 10^4$ K and $N_e = 10^4$ cm^{-3} (Brocklehurst 1971). In AGNs, however, the harder photoionizing spectrum results in a large transition zone, or partly ionized region, in which H^0 coexists with H^+ and free electrons. In this zone collisional excitation is also important in addition to recombination collisional excitation (Ferland and Netzer 1983; Halpern and Steiner 1983). The main effect of collisional excitation is to enhance Hα. The higher Balmer lines are less affected because of their larger excitation energies and smaller excitation cross sections. For the intrinsic ratio for AGNs, we have adopted $I(H\alpha)/I(H\beta) = 3.1$, in agreement with the results of recent photoionization models (Ferland and Netzer 1983, Péquignot 1984) and observational determinations (Gaskell 1984; Gaskell and Ferland 1984). This represents a change from much of the earlier Lick AGN research, in which the recombination value 2.85 was used as a first approximation.

Using this method with intrinsic ratios $I(H\alpha)/I(H\beta) =$ 2:85 for H II region galaxies, $I(H\alpha)/I(H\beta) = 3.1$ for Seyfert 2, narrow-line radio galaxies and LINERs, and whichever of these two values is consistent with their position in our classification diagrams for NELGs, we recorrected for interstellar extinction all the line ratios measured by Koski (1978), Costero and Osterbrock (1977) and Shuder and Osterbrock (1981). We did not find any systematic differences between the line ratios dereddened in this way using only the measured value of $F(H\alpha)/F(H\beta)$, and the line ratios as previously dereddened using the maximum number of Balmer lines possible [but with $I(H\alpha)/I(H\beta) = 3.1$ for active galaxies]. The measured ratios of Balzano (1983) were also corrected for the reddening using the same method. French (1980) and Dinerstein and Shields (1986) used a similar reddening correction procedure, and McCall, Rybski, and Shields (1985) used the same method but with the very nearly identical reddening curve of Schild (1977). Consequently, we used the dereddened line ratios from these three papers directly without any modification. Keel (1983) determined the internal reddening of the galaxies he measured by determining the value of $E(B-V)$ that gave the best-fitting synthesis (continuum shape and depth of 6180 Å TiO band). His reddening-corrected line ratios were also included in this study without modification.

All the measured line ratios presented in Tables 2–4 have been corrected for reddening using the procedure described above. The corrected values are listed in the second line for each object in these tables, along with the amount of extinction c.

e) *Results*

In Figures 1–3 the reddening-corrected ratios [O III] λ5007/Hβ are plotted for all the objects as functions of [N II] λ6583/Hα, [S II] (λ6716 + λ6731)/Hα, and [O I] λ6300/Hα, respectively. In these three diagrams narrow-line AGNs (Seyfert 2 galaxies, narrow-line radio galaxies, or LINERs) are plotted as filled symbols of various forms (as indicated in the key to Fig. 1), while H II regions in external galaxies, starburst galaxies, and H II region galaxies are plotted as open symbols (as indicated in the key to Fig. 2), and objects previously published as NELGs, i.e., emission-line galaxies that may be either LINERs or H II region galaxies, are plotted as asterisks. Arrows on data points indicate lower or upper limits. The size of each plotted point gives an

TABLE 3

MEASURED AND CORRECTED EMISSION-LINE RATIOS FOR SEYFERT GALAXIES AND SEYFERT GALAXY CANDIDATES: CCD SPECTROGRAPH, 3 METER TELESCOPE

Mrk	$\log \frac{[O\ III]}{H\beta}$	$\log \frac{[N\ II]}{H\alpha}$	$\log \frac{[S\ II]}{H\alpha}$	$\log \frac{[O\ I]}{H\alpha}$	$\log \frac{H\alpha}{H\beta}$	z,[a] c	Class
111[b]	+0.14	−0.61	−0.57	−1.42	0.82	0.0124, 1.09	NELG
	+0.10	−0.61	−0.59	−1.38	0.45		
111[b] comp	+0.36	−0.69	−0.53	−1.30	0.70	0.0119, 0.73	NELG
	+0.33	−0.69	−0.55	−1.27	0.45		
432 W	+0.10	−0.68	−0.51	−1.43	0.63	0.0108, 0.52	NELG
	+0.08	−0.69	−0.52	−1.41	0.45		
490 A+B[c]	+0.53	−1.01	−0.66	−1.66	0.52	0.0086, 0.20	NELG
	+0.52	−1.01	−0.67	−1.65	0.45		
490 C[c]	+0.86	−1.68	−1.24	−1.80	0.43	0.0088, 0.00	NELG
	+0.86	−1.68	−1.24	−1.80	0.45		
522	+0.51	−0.03	−0.53	−1.17	0.87	0.0316, 1.13	S2
	+0.47	−0.04	−0.56	−1.13	0.49		
540	−0.38	−0.20	−0.94	−1.35	0.87	0.0703, 1.13	NELG
	−0.42	−0.20	−0.97	−1.31	0.45		
724	+0.69	−1.12	−1.11	...	0.42	0.0034, 0.00	NELG
	+0.69	−1.12	−1.11	...	0.45		
930	+0.68	−1.30	−0.82	−1.58	0.58	0.0195, 0.37	SBG
	+0.67	−1.30	−0.82	−1.57	0.45		
1040[b] comp	+0.36	−0.67	−0.49	−1.40	0.79	0.0160, 1.01	NELG
	+0.33	−0.68	−0.52	−1.36	0.45		
1125+581[d]	+0.91	−0.08	−0.43	...	0.95	0.0513, 1.38	S2
	+0.86	−0.09	−0.47	...	0.49		
1133+572[d]	+1.00	+0.13	−0.39	−1.08	0.69	0.0506, 0.61	S2
	+0.98	+0.13	−0.40	−1.06	0.49		
1212	−0.47	−0.21	−0.64	−1.58	0.90	0.0408, 1.32	NELG
	−0.52	−0.21	−0.67	−1.53	0.45		
1315[e]	+0.75	−1.60	−1.28	−1.70	0.64	0.0023, 0.55	H II
	+0.73	−1.60	−1.29	−1.68	0.45		
1388[b]	+1.05	−0.48	−0.84	−0.94	0.66	0.0213, 0.49	S2
	+1.03	−0.48	−0.85	−0.92	0.49		
1414	−0.31	−0.40	−0.56	−1.61	0.85	0.0150, 1.18	NELG
	−0.36	−0.40	−0.58	−1.57	0.45		
NGC 4670	+0.48	−1.06	−0.80	−1.73	0.53	0.0026, 0.24	NELG
	+0.47	−1.06	−0.81	−1.72	0.45		
NGC 7212	+1.07	−0.14	−0.34	−0.78	0.44	0.0265, 0.00	S2
	+1.07	−0.14	−0.34	−0.78	0.49		

[a] The uncertainty in z varies from ± 0.0002 to ± 0.0005.

[b] Other names: Mrk 111 = Arp 300, Mrk 111 comp = Arp 300, Mrk 1040 comp = NGC 931.

[c] Published data: Mrk 490: De Robertis and Osterbrock 1986; Mrk 1388: Osterbrock 1986.

[d] Second Byurakan Spectral Sky Survey Objects (Markarian, Lipovitsky, and Stepanian 1983): Mrk II 1125+581 = SBS 1125+581, Mrk II 1133+572 = SBS 1133+572.

[e] This is an outlying H II region of NGC 4204.

TABLE 4

MEASURED AND CORRECTED EMISSION-LINE RATIOS FOR STARBURST GALAXIES: IMAGE-DISSECTOR SPECTROGRAPH, 1 METER TELESCOPE

Mrk	$\log \frac{[O\ III]}{H\beta}$	$\log \frac{[N\ II]}{H\alpha}$	$\log \frac{[S\ II]}{H\alpha}$	$\log \frac{[O\ I]}{H\alpha}$	$\log \frac{H\alpha}{H\beta}$	z,[a] c	Class
326[b] ...	−0.39:	−0.29	−0.50	≤ −1.27	0.65	0.0116, 0.59	SBG
	−0.41:	−0.30	−0.52	≤ −1.24	0.45		
363[b] ...	−0.01	−0.61	−0.50	−1.25	0.73	0.0096, 0.82	SBG
	−0.04	−0.62	−0.52	−1.21	0.45		
529[b] ...	+0.48	−0.69	−0.52	≤ −1.45	0.74	0.0118, 0.86	SBG
	+0.44	−0.69	−0.54	≤ −1.41	0.45		
545[b] ...	−0.32:	−0.24	−0.55	≤ −1.18	0.54	0.0150, 0.27	SBG
	−0.33:	−0.25	−0.56	≤ −1.16	0.45		
909	+0.16	−0.75	−0.40	≤ −1.10	0.46	0.0143, 0.01	SBG
	+0.16	−0.75	−0.40	≤ −1.10	0.45		
1002[b] ..	−0.36	−0.40	−0.51	≤ −1.31	0.51	0.0104, 0.16	SBG
	−0.37	−0.40	−0.51	≤ −1.30	0.45		

[a] The uncertainty in z varies from ±0.0002 to ±0.0005.

[b] Other names: Mrk 326 = NGC 7677, Mrk 363 = NGC 694, Mrk 529 = NGC 7532, Mrk 545 = NGC 23, Mrk 1002 = NGC 632.

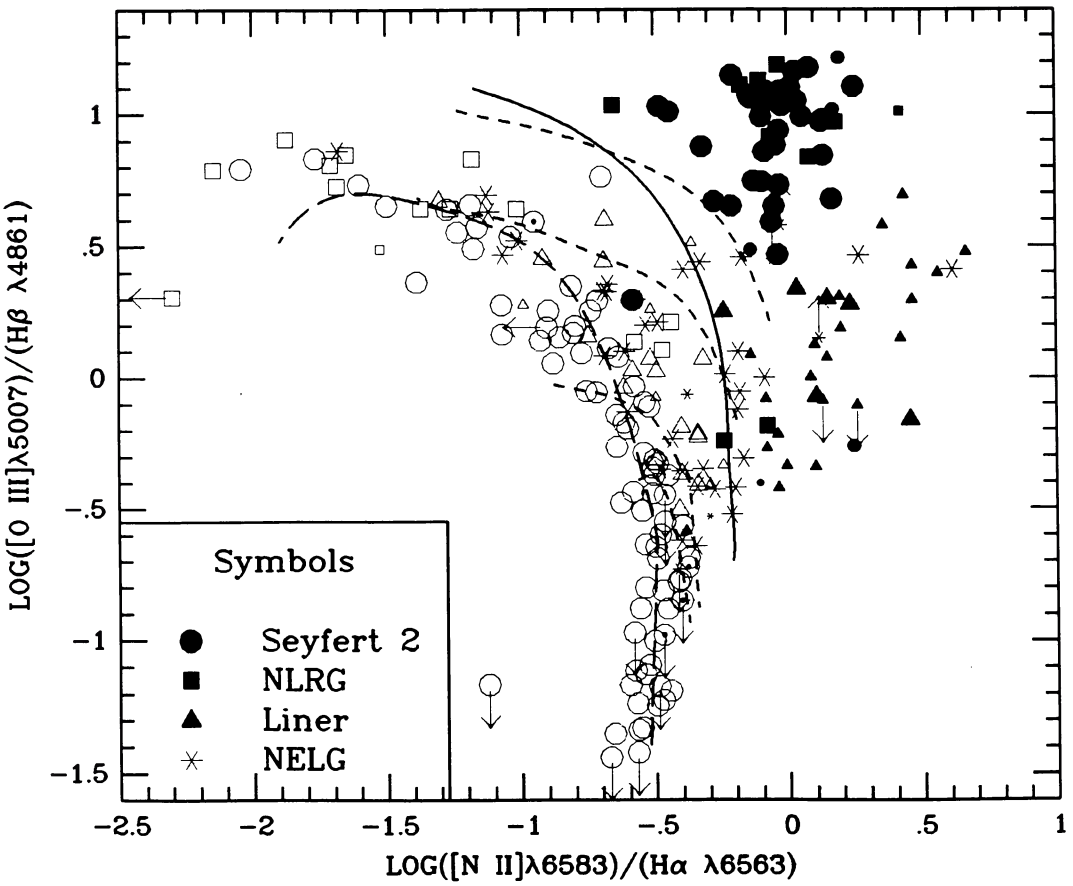

FIG. 1.—Reddening-corrected [O III] λ5007/Hβ vs. [N II] λ6583/Hα intensity ratios. Symbols for types of objects are as shown in keys to this figure and Fig. 2. Four short-dashed lines are H II region models of Evans and Dopita (1985) for $T_* = 56{,}000$, 45,000, 38,5000, and 37,000 K from the top to bottom respectively. Long-dashed curve represents H II region models of McCall, Rybski, and Shields (1985). Solid curve divides AGNs from H II region–like objects.

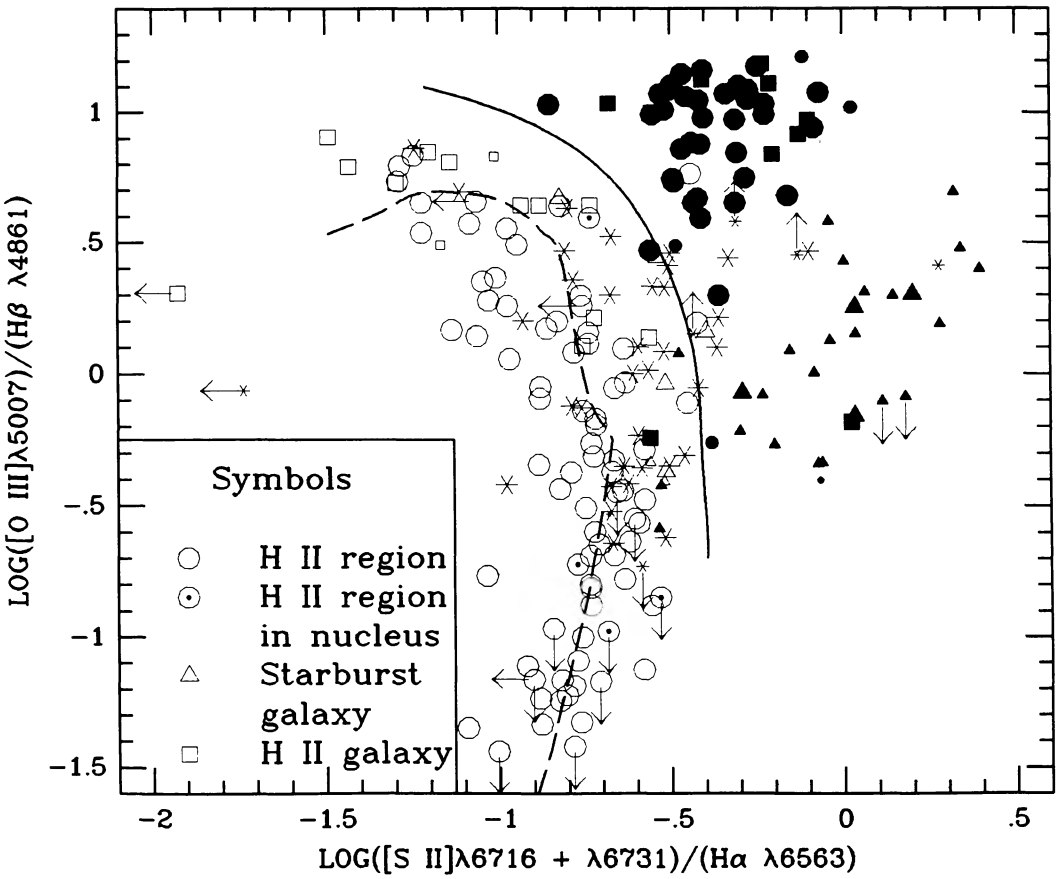

FIG. 2.—Reddening-corrected [O III] λ5007/Hβ vs. [S II] (λ6716 + λ6731)/Hα intensity ratios. Symbols and curves as in Fig. 1.

indication of its uncertainty; large symbols represent objects for which both plotted line ratios are accurate to better than ±30%, while smaller symbols represent objects where either one of the line ratios is uncertain by more than 30%.

The uncertainty of the line ratios depends on many factors, such as the strength of the lines, the type of instrument used, and whether or not the lines are blended with other lines. Costero and Osterbrock (1977), Koski (1978), French (1980), Shuder and Osterbrock (1981), Keel (1983), and Osterbrock and Dahari (1983; line ratios measured in the present paper) all used the IDS system at Lick Observatory, which is known by experience to give line ratios of the stronger lines with an accuracy of about ±10%, and of the weaker lines of about ±20%. These uncertainties are also typical of the values stated by McCall, Rybski, and Shields (1985) and Dinerstein and Shield (1986). Working at somewhat lower spectral resolution, Balzano (1983) estimated the uncertainty of her measured line ratios to be 20%–30%. The errors of the line ratios of objects with the CCD grism spectrograph at the Shane telescope are less well known but appear to be only slightly larger than those obtained with the IDS (Osterbrock and De Robertis 1985). The necessity of deblending Hα from [N II] λλ6548, 6583 usually causes the estimated error of Hα to be roughly equal to that of Hβ, in spite of the greater strength of Hα (Koski 1978). Another source of uncertainty that can be quite important in some objects results from the underlying integrated stellar absorption component. To remove it from the emission-line spectrum is not straightforward. If the emission lines are weak and the galaxy absorption-line spectrum is moderately strong, the process can be highly subjective. In order to minimize this source of uncertainty in our newly analyzed galaxies, we have preferentially measured objects with spectra in which the emission-line intensities (particularly Hβ) were not greatly affected by the underlying stellar component.

The sample used in this study is not complete in any sense. The distributions of data points in Figures 1–3 are certainly affected by selection effects. Only objects with emission lines strong enough to measure are included in these diagrams. Figure 3 includes fewer data points than the other two figures because only very few measurements of [O I] λ6300 have been published for H II region galaxies. This situation should be improved in the near future. Some regions of the diagram seem deserted: we do not have any objects with [O III] $\lambda 5007/H\beta < 0.3$ and [N II] $\lambda 6583/H\alpha > 0.5$, or [S II] $(\lambda 6716 + \lambda 6731)/H\alpha > 0.5$.

These empty regions in the diagrams may be due to selection effects. Galaxies with very low ionization tend to have all their emission lines very weak. In such cases the difficulty in removing the stellar absorption spectrum would prevent us from making reliable measurements of line fluxes (especially Hβ). Likewise, the seemingly "bimodal" distribution of AGNs

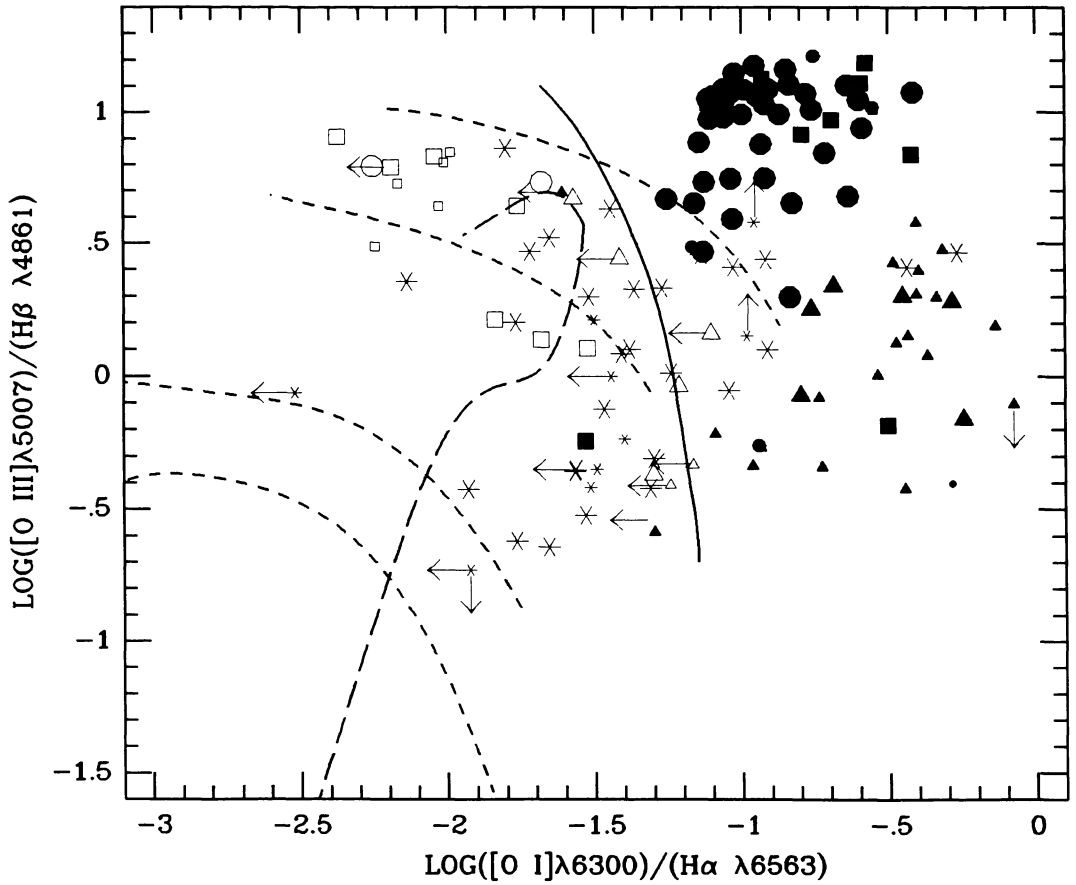

FIG. 3.—Reddening-corrected [O III] λ5007/Hβ vs. [O I] λ6300/Hα intensity ratios. Symbols and curves as in Figs. 1 and 2.

(Seyfert 2 and radio galaxies with high [O III] λ5007/Hβ on the one hand versus LINERs with low [O III]/Hβ on the other) very probably results from fewer measurements of objects with intermediate [O III] λ5007/Hβ.

The diagrams of Figures 1–3 show a clear separation between H II region–like objects and narrow-line AGNs. The distribution of NELGs, however, is not like the distribution of either class of objects. Instead, some NELGs are clearly H II region galaxies, while others are narrow-line AGNs. The ratio [O III] λ5007/Hβ alone is a good indicator of the type of object, because there is a considerable overlap of the value of [O III] λ5007/Hβ for H II region–like objects with the value of this same ratio for narrow-line AGNs.

When we compare Figure 1 with Figure 5 of BPT, we note that the dichotomy between high-ionization narrow-line AGNs ([O III] λ 5007/Hβ ≥ 3) and low-ionization narrow-line AGNs has been reduced considerably. This is another indication that LINERs probably constitute the lower part of a sequence of ionization that extends up to the Seyfert 2 and narrow-line radio galaxies (see § III*b*). Finally, in Figures 1–3 there is no systematic difference between the positions of the H II region *galaxies* and the H II *regions* of McCall, Rybski, and Shields (1985). The low-luminosity galaxies of French (1980) occupy the high-ionization end of this H II region galaxy sequence, while the starburst galaxies of Balzano (1983) are located near the low-ionization end of it.

A few objects have line ratios atypical of their class. They will be discussed in § IV, where we will present a more quantitative description of the difference between H II region–like objects and narrow-line AGNs.

III. MODELS

In this section we will discuss models photoionized by the radiation emitted from hot stars and by a power-law continuum. Shock-heating models will be discussed briefly because this process may also play a role (though probably not a dominant one) in LINERs. The goal of this section is to provide as firm a theoretical framework for distinguishing H II region–like objects from narrow-line AGNs as is possible with available models. The classification presented in the next section is based on the observational data interpreted on the basis of the models.

a) *Photoionization by Hot Stars*

In BPT, the simplified models of Searle (1971) were used to represent the calculated line ratios of H II regions in their diagrams. Although these models give relatively good predictions in terms of line ratios, recent models have been shown to be much more useful for studying H II regions in more detail (particularly their composition).

Evans and Dopita (1985) have published an extensive, homogeneous grid of photoionization models with conditions appropriate to observed H II regions. Using recent atomic data, they computed models of dust-free, steady state spherically symmetric nebulae with unit filling factor and uniform density ($N_H = 10$ cm^{-3}; they note that, in the low-density limit, the effect on the spectrum of changing N_H by a factor D is equivalent to changing the mean ionization parameter U by a factor $1/D$). The stellar-atmospheric models of Hummer and Mihalas (1970), with $\log g = 4.0$, were used to calculate the input spectrum of the ionizing radiation. The spatial integration was continued until N_{H^+}/N_H was smaller than 1%. Evans and Dopita (1985) developed extensive grids of models with different ionization parameters U and stellar effective temperatures T_*. (The cluster of stars was replaced by a single ionizing star of effective temperature T_* yielding the cluster-average emitted photon energy. T_* corresponds to a temperature close to the effective temperature of the hottest star in the cluster.) The metal abundances in the model stellar atmospheres matched those in the model nebulae. Evans and Dopita's results for model of solar metallicity are shown as short-dashed lines in Figures 1 and 3. [They did not give explicit predicted intensities for [S II] (λ6716 + λ6731).] In each diagram the predicted line ratios are shown for four different stellar temperatures. The ionization parameter U varies along each curve from $10^7/c$ to $10^9/c$, where c is the speed of light in centimeters per second.

The behavior of the curves in Figure 1 can be understood qualitatively as follows. The number of photons capable of ionizing O^+ depends on U and T_*; it decreases as we progress from high to low U and T_*. Consequently, the size of the O^{++} zone and the total [O III] emission also decrease. For a given T_*, as U decreases, the zone containing a singly ionized species such as N^+ therefore becomes steadily larger and eventually fills the whole volume of the ionized H^+ zone. The curves in Figure 3 can be interpreted similarly, comparing this time the size of the thin, partly ionized transition zone (in which [O I] λ6300 is emitted) with the [O III] emission zone. The models with the hottest T_* have the largest fraction of high-energy photons, and thus the largest transition regions.

Using their diagnostic diagrams of [O I] λ6300/[O III] λ5007 versus [O II] λ3727/[O III] λ5007 and the data sample used by BPT, augmented by the spectrophotometry of McCall (1982), Evans and Dopita (1985) concluded that H II regions are characterized by a considerable range in U and an effective stellar temperature $T_* \approx 41{,}000$ K, with relatively small scatter. They interpreted this behavior as resulting from the fact that the stars principally responsible for the ionizing photons are those located approximately at the main-sequence turnoff, and that theoretical isochrones for clusters of typical H II region ages, $4\text{–}8 \times 10^6$ years, have main-sequence turnoffs which occur at nearly constant temperature. We cannot comment on the conclusion because there are no measurements of [O I] λ6300 for the H II regions of the later data sample (McCall, Rybski, and Shields 1985) that we used. We note, however, that if H II region–like galaxies are characterized by a single stellar effective temperature, it seems to be at least $T_* \geq 45{,}000$ K, that is, 4000 K higher than the typical stellar temperature of ordinary H II regions. We also note that many of the so-called NELGs fall in a region characterized by lower effective stellar temperatures. These particular "NELGs" evidently represent a selection of lower ionization H II region galaxies.

Next we consider the [O III] λ5007/Hβ versus [N II] λ6583/Hα diagram of Figure 1. There is a better agreement between the models and the data if the model is translated to weaker [N II] line strength by about 0.1 dex (Evans and Dopita 1985). To maintain that the distribution of H II region–like objects is characterized by a single effective stellar temperature ($T_* \approx 41{,}000$ K), it is necessary to assume an anticorrelation between ionization parameter and metallicity. On this picture for large U the metallicity is smaller than the solar value, the line opacity in the model stellar atmospheres is less efficient, and hence there are more far-ultraviolet photons, resulting in a larger O^{++} zone and a smaller N^+ zone. We thus expect, for high values of U, a larger [O III] λ5007/Hβ and a smaller [N II] λ6583/Hα than predicted by the model with $Z = Z_\odot$. At small U, the opposite is expected (Evans and Dopita 1985).

Next we discuss the H II region models of McCall, Rybski, and Shields (1985). The physics of these models is summarized in their Table 11. The behaviors of [O III] λ5007/Hβ as a function of [N II] λ6583/Hα, of [S II] (λ6716 + λ6731)/Hα, and of [O I] λ6300/Hα are shown as long-dashed lines in Figures 1, 2, and 3, respectively.

The model is a spherical nebula of uniform density ($N_H = 140$ cm^{-3}, the average value obtained for all theory objects from the [S II] ratio). McCall, Rybski, and Shields (1985) show that the emission-line spectra of H II regions form a one-parameter sequence with the O abundance as the fundamental parameter. The value of every other parameter is determined by it. In order to reproduce the range of the spectral properties observed in their sample, the abundance ratio O/H was assumed to vary from less than 0.5 solar to more than 3.5 times solar. McCall, Rybski, and Shields (1985) assumed that the effective stellar temperature varies as a power law in O/H when $O/H < 1.9(O/H)_\odot$, but is constant for higher O/H. The entire range of the effective stellar temperature is relatively small, 38,500–47,000 K, and thus is not inconsistent with the conclusion of Evans and Dopita (1985). McCall, Rybski, and Shields (1985) assume that N/H varies as $(O/H)^2$. On the basis of observation of high-ionization H II regions (low metallicity), a base value of N/H of 10^{-6} was chosen. The abundances of all other heavy elements were assumed to vary linearly with O/H, while He was held fixed at the "solar" value.

In Figures 1–3 we see that these models provide a good fit to the H II region galaxies of our sample, as well as to the H II regions for which it was developed. It appears, however, that the models have difficulty accounting for the [O I] λ6300/Hα ratios of the H II region galaxies plotted in Figure 3. [O I] λ6300 was not measured for the H II regions by McCall, Rybski, and Shields (1985).

b) Photoionization by a Power-Law Continuum

The source of heating and ionization in Seyfert 2 galaxies and in narrow-line galaxies appears to be a "power-law" nonthermal continuum (Koski 1978). In the last decade many

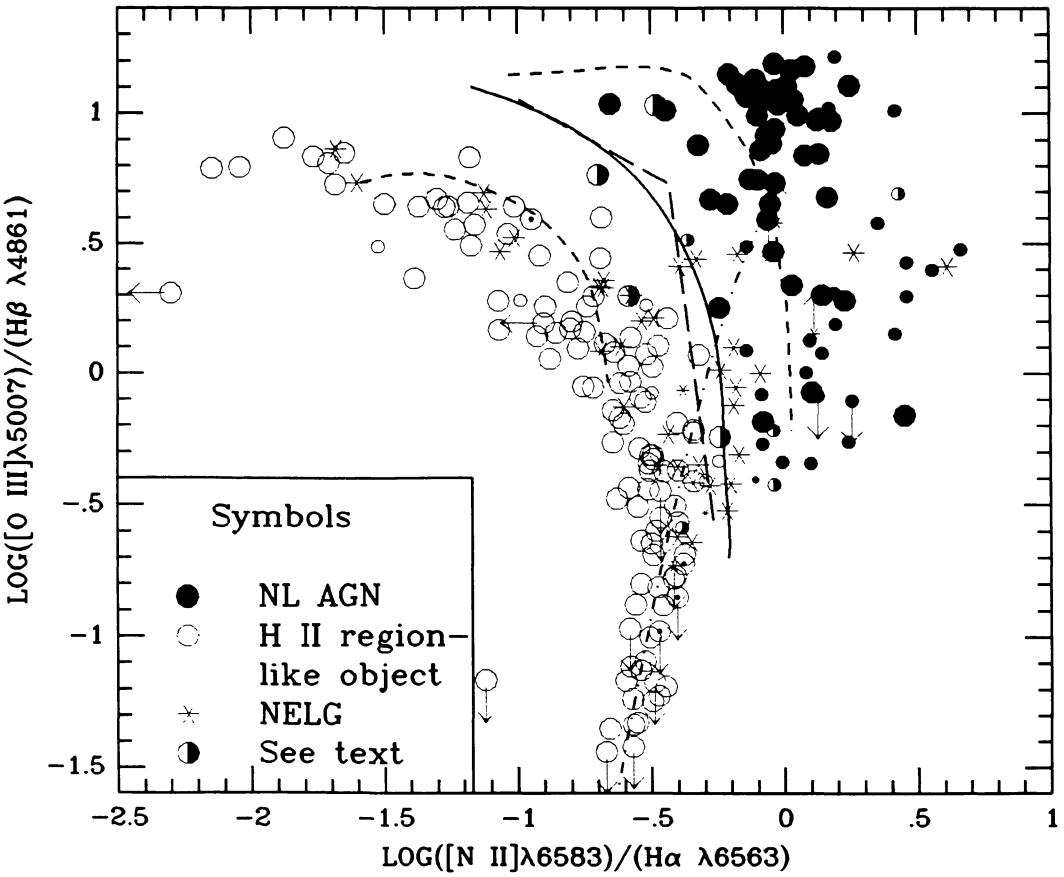

FIG. 4.—Reddening-corrected [O III] λ5007/Hβ vs. [N II] λ6583. Hα intensity ratios. Symbols for types of objects are as shown in key to figure. Short-dashed curves are power-law models of Ferland and Netzer (1983) for solar and 0.1 times solar abundances (upper and lower, respectively). Ionization parameter varies along curves from $10^{-1.5}$ to 10^{-4}. Long-dashed line is composite, two-component ($N_e = 10^2$ and 10^6 cm^{-3}) model of Stasinska (1984*b*). Ionization parameter varies along curve from 10^{-2} to 10^{-4}. Dot-dash curve represents shock-wave models of Shull and McKee (1979). Shock velocity varies along the curve from less than 80 to 130 km s^{-1}. Solid curve divides AGNs from H II region–like objects.

attempts have been made to model Seyfert galaxies. To the present time the models have reached only partial agreement with the observational data. Our incomplete understanding of the central energy sources in AGNs is at least partly responsible for this situation. The major improvements of current models over earlier ones (see Davidson and Netzer 1979 for a review) have come in part from the inclusion of important X-ray ionization effects (such as inner-shell ionization, Auger effects, secondary ionization by suprathermal electrons, and so on) in the calculations and from better atomic data. Also, the earlier calculations failed to reproduce the strengths of some of the low-ionization lines (Koski 1978) because they did not include important charge-transfer reactions.

In order to understand the distribution of the narrow-line AGNs in our diagrams, we have compared the same observational data with recent photoionization power-law model calculations in Figures 4–6. In these three diagrams all the same data are plotted, but here all AGNs are plotted as filled circles, and all H II region–like objects as open circles. The NELGs are again plotted as asterisks, and the few special or peculiar objects discussed in the text as half-filled circles. Ferland and Netzer (1983, hereafter FN) published a set of models with a large range of ionization parameter U. Using these results, the predicted behavior of [O III] λ5007/Hβ is plotted as a function of [N II] λ6583/Hα for two metal abundances as short-dashed lines in Figure 4. The high-ionization line [O III] λ5007 decreases in strength with decreasing U, while the low-ionization line [N II] λ6583 increases in strength.

Figures 5 and 6 show the same series of models in the other two diagrams, plotting [O III] λ5007/Hβ as a function of [S II] (λ6716 + λ6731)/Hα and [O I] λ6300/Hα, respectively. Most of the observed narrow-line AGNs fall between the solar abundance and the 0.1 solar abundance models. Hence, an interpretation based on these models suggests that the observed narrow-line AGNs are characterized by metal abundances that are on the average lower than solar. FN arrived at essentially this conclusion using a somewhat smaller sample of Seyfert 2 galaxies, narrow-line radio galaxies, and LINERs, together with the narrow-line regions of some broad-line objects (Seyfert 1 galaxies, broad-line radio galaxies, QSOs). The narrow-line AGNs of our sample are matched by models with a large range of ionization parameters, from $U \approx 10^{-1}$ to $U \approx 10^{-3.5}$ for the Seyfert 2 galaxies and $U \lesssim 10^{-3.5}$ for

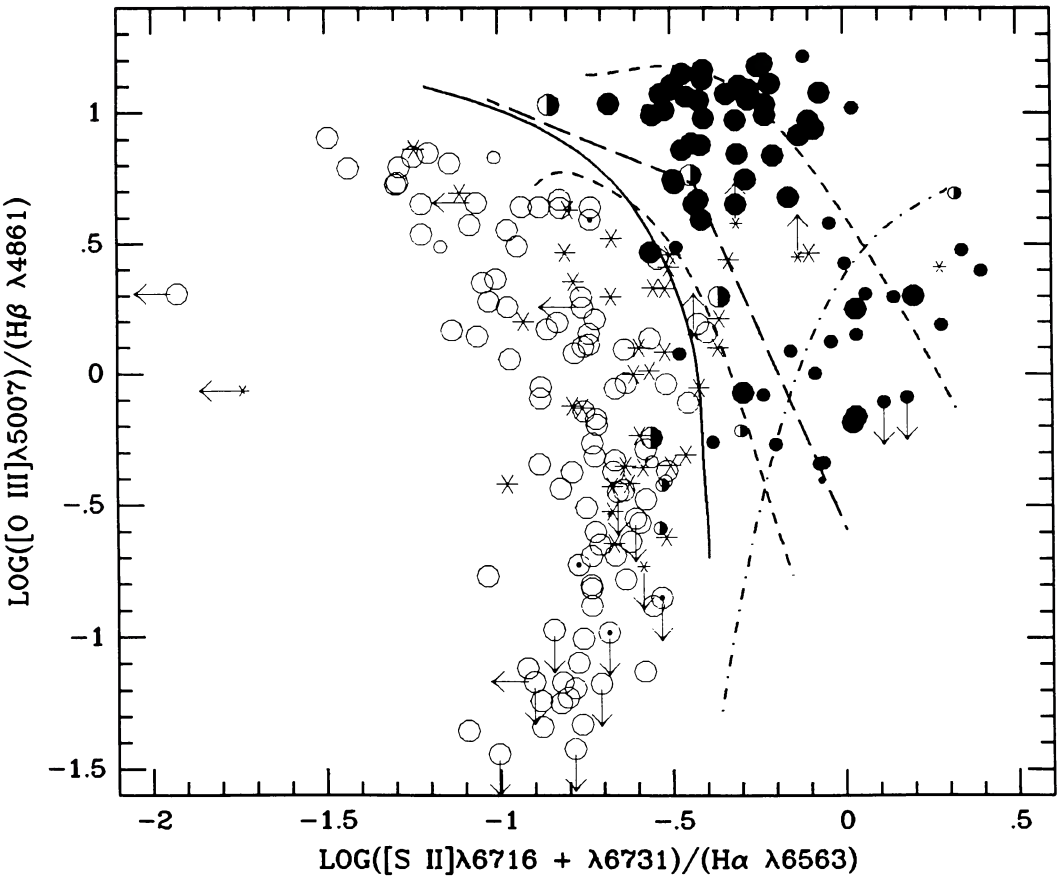

FIG. 5.—Reddening-corrected [O III] λ5007/Hβ vs. [S II] (λ6716+λ6731)/Hα intensity ratios. Symbols and curves as in Fig. 4.

LINERs. This sequence of models also seems to agree with the [N II] λ6583/Hα ratios of Figure 4, but with the higher metallicities. As FN noted, this suggests that the depletion factor of N is not as large for O and S.

Stasinska (1984*a*, *b*) investigated the consequences of a change of the spectral index α of the assumed photoionizing power-law spectrum $\nu^{-\alpha}$ on the preceding line ratios. As α becomes smaller, ionization by X-ray photons becomes more important and [O I] λ6300/Hα, [S II] (λ6716+λ6731)/Hα, [N II] λ6583/Hα, and (to a lesser extent) [O III] λ5007/Hβ all become larger. Since the average (horizontal) position of Seyfert 2 nuclei and narrow-line radio galaxies does not seem to be systematically different from the average position of LINERs (with respect to the same models), we cannot draw any conclusions as to whether or not the ionizing continuum in high-ionization AGNs is flatter than in low-ionization AGNs (Binette 1985). A difference in heavy-element abundances between high- and low-ionization AGNs could smear out any observable effects of the form of the spectrum (see below).

The models of FN and of Stasinska (1984*a*) are one-component models that do not include possible density-stratification effects. Recent observations indicate a correlation between the line widths of forbidden lines and the critical densities of their upper levels for collisional de-excitation in Seyfert 2 galaxies (De Robertis and Osterbrock 1986). This can be explained only if the photoionized gas has a range of densities. Several photoionization models that include density stratification have been published in recent years (Stasinska 1984*b*; Péquignot 1984; Binette 1985; Ferland and Osterbrock 1986). Although the predictions of these models agree qualitatively with those of single-component models, important differences are also apparent. In particular, estimates of the abundances of heavy elements based on strong optical lines in AGNs with a wide range of densities will be *underestimated* if the observations are compared with the predicted line intensities from a one-component (low-density) model. The strong observed nebular lines begin to be affected by collisional de-excitation at various densities in the range 10^3–10^5 cm^{-3}. Models with a uniform density of 10^3 cm^{-3} (or, similarly, models with constant pressure and initial density of 10^3 cm^{-3} such as those of FN) assume the relevant lines to be emitted at their maximum efficiency; if they actually are emitted in less favorable conditions because of stratification, then the abundances (with respect to H) will automatically be underestimated (Péquignot 1984).

In order to investigate semiquantitatively the effects of density gradients in narrow-line AGNs, we have used one of the composite models of Stasinska (1984*b*). In Figures 4–6 the predictions of these models are represented by the long-dashed curves. The composite models include two components of different densities ($N_1 = 10^2$ cm^{-3}, $N_2 = 10^6$ cm^{-3})

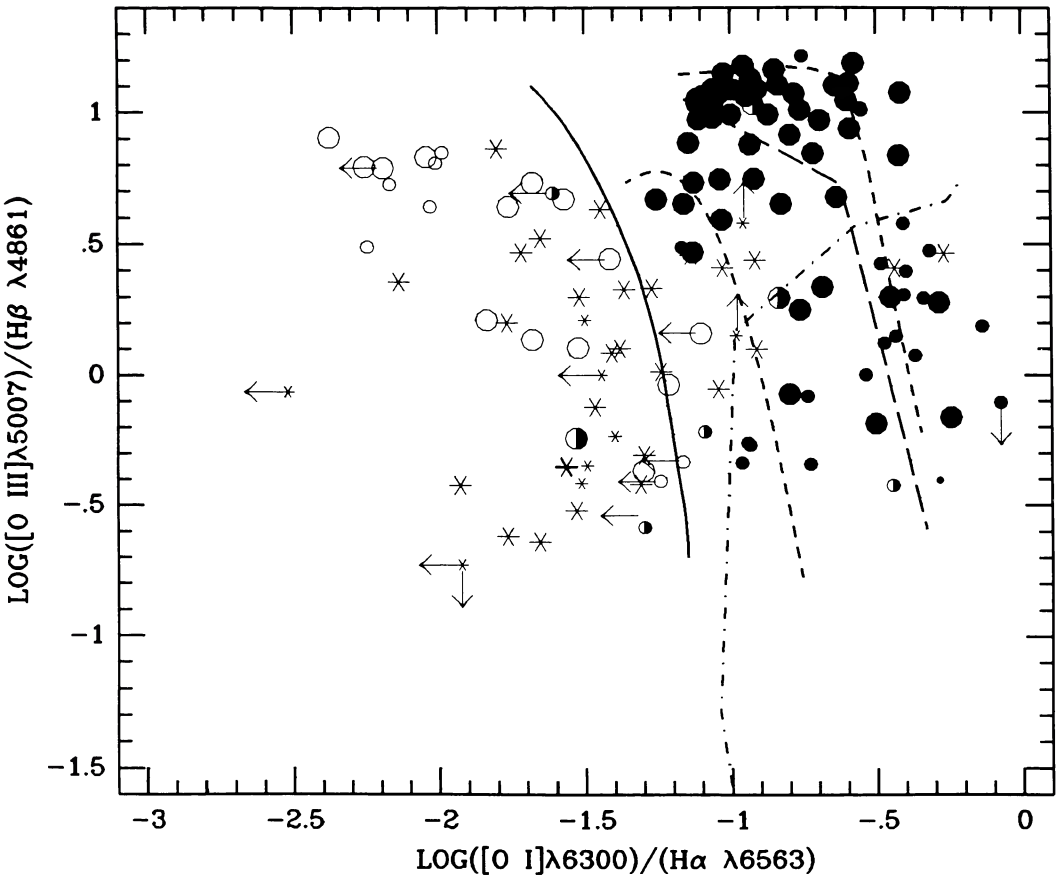

FIG. 6.—Reddening-corrected [O III] λ5007/Hβ vs. [O I] λ6300/Hα intensity ratios. Symbols and curves as in Fig. 4.

with the same ionization parameter, which varies along the curve from $U=10^{-2}$ to $U=10^{-4}$. The abundances are assumed to be solar. Although these models are undoubtedly a highly simplified representation of the stratification in narrow-line AGNs, we see that the abundances of the heavy elements can be underestimated by quite large factors. This is especially true for the [O III] λ5007/Hβ versus [S II] (λ6716 + λ6731)/Hα diagram, where the metallicity estimated from the two-component models is greater than the solar value, while from the models of FN it would clearly be less than solar. The [O I] λ6300/Hα predictions from the model of Stasinska do not greatly differ from the models of FN. It also appears that there are larger variations of [N II] λ6583 among the LINERs than among the Seyfert 2 galaxies. This may indicate a larger variation of the N abundance in low-ionization AGNs than in high-ionization ones.

Finally, it is important to mention that these comments concerning the abundances of heavy elements in AGNs are only first-order indications, because the models used here, although better than the one-component models, are still too crude to be reliable for accurate abundance analyses. Binette (1985) has investigated the metal abundances in LINERs using photoionization models with density stratification (Gaussian centered at the origin). He found that the best choice of a power-law photoionizing continuum had $\alpha=2$, and deduced that the metallicity in the LINERs is approximately solar. Estimates of the average heavy-element abundances in narrow-line AGNs are at present very uncertain. More accurate estimates will be possible only with more realistic photoionization models.

c) *Shock Heating*

In the interests of completeness, shock heating should be considered as an alternative ionization mechanism in narrow-line AGNs. Many models of interstellar shocks have been published. Dopita (1976, 1977) and Raymond (1979) calculated plane-parallel models in which the ionization state of the preshock gas was essentially a free parameter. Shull and McKee (1979) improved on this assumption by constructing theoretical models in which they paid special attention to the transfer of ionizing radiation and to the effects of the emergent ultraviolet radiation on the ambient preshock gas.

In a subset of seven models they studied the effects of varying the shock velocity without varying the preshock conditions. In Figures 4–6 the predicted intensity ratios obtained from this series of models are plotted as dot-dash lines. The shock velocity increases along these curves from less than 80 to 130 km s^{-1}. [O III] λ5007/Hβ increases rapidly with shock velocity, while [N II] λ6583/Hα, [S II] (λ6716+ λ6731)/Hα, and [O I] λ6300/Hα increase only slightly, the latter two actually decreasing as the shock velocity changes from 60 to 80 km s^{-1}, and then increasing again.

Since there is no doubt that the emission lines in high-ionization AGNs are produced by photoionization, we direct our attention to the lower-ionization AGNs (LINERs). If these objects are shock-heated, the shock velocity must be at least 80 km s^{-1}. Since the sample is probably incomplete for log [O III] $\lambda 5007/H\beta \lesssim -0.25$, additional data will probably lower this limit and thus the lower limit of shock velocity. Most of the LINERs have [N II] $\lambda 6583/H\alpha$ larger than the predicted values from the "standard" model of Shull and McKee (1979). The discrepancy between observations and theory may be diminished if the N abundance is larger than solar. The same interpretation may apply to O and (to a smaller extent) to S.

Although models photoionized by a power-law spectrum (FN; Stasinska 1984*b*, and others) give a better fit to the observed line intensities of LINERs than shock-heating models, it is impossible to choose between the two excitation mechanisms on the basis of Figures 4–6 alone. Other tools must be used to identify securely the source of ionization in LINERs. Early papers interpreted individual "LINERs" as shock-heated on the basis of specific line ratios such as [O III] $\lambda 4363/\lambda 5007$ (Koski and Osterbrock 1976; Fosbury *et al.* 1978). More recent papers have attacked this interpretation. Keel and Miller (1983) and Rose and Tripicco (1984) discuss the large uncertainties in the determination of the [O III] $\lambda 4363/\lambda 5007$ ratio. Important sources of error are the absorption features due to CN and Hγ near [O III] $\lambda 4363$ and, at low redshift, the Hg I $\lambda 4358$ night-sky light-pollution emission line. The high-ionization line He II $\lambda 4686$, observed even if only very weakly, is an indicator of photoionization by a power-law spectrum rather than shock heating in galaxies with ionization of O as low as in LINERs (Osterbrock and Dahari 1983). Goodrich and Keel (1986) discuss the possible detection of a nonthermal UV continuum in NGC 4579. Finally, the presence of weak, broad wings to the narrow emission lines in many LINERs, including even NGC 1052 (Heckman 1980; Stauffer 1982; Keel 1983; Filippenko and Sargent 1985), strongly favors the continuity with Seyfert galaxies and hence the photoionization interpretation. Thus, it seems increasingly likely that the dominant excitation mechanism in LINERs is photoionization by a power-law continuum, and that it is justified to classify them as narrow-line AGNs similar to Seyfert 2 galaxies and narrow-line radio galaxies. On the other hand, there are many signs of shock-wave heating in extended ionized regions in apparently merged and distorted galaxies.

IV. CLASSIFICATION OF NARROW-EMISSION-LINE GALAXIES

The physical difference that distinguishes a narrow-line AGN from an H II region–like galaxy is the photoionizing continuum. In narrow-line AGNs the ionizing radiation is well approximated by a power-law continuum $\nu^{-\alpha}$ with spectral index $\alpha \sim 1.0$–1.5 (see, for example, Koski 1978; Ferland and Osterbrock 1986) or by a combination of two such power laws, with $\alpha \approx 0.5$ at higher energies (see, for example, Kwan and Krolik 1981). In H II regions the ionization is due to UV photons emitted by hot OB stars. So, in contrast with H II region–like objects, narrow-line AGNs have a significant fraction of their energy in the X-ray domain. These X-ray photons have important consequences for the ionization structure of the nebula. Because the absorption cross sections of H^0, He^0, He^+, and all other ions decrease rapidly with increasing energy, kilovolt X-rays penetrate deeply into the predominantly neutral region. There they produce a large partly ionized zone, with characteristic fraction of ionized hydrogen $H^+/H \sim 0.2$–0.4 (see, e.g., Weisheit, Shields, and Tarter 1981; Netzer 1980; Osterbrock 1984). These results apply qualitatively to Seyfert 2 galaxies, narrow-line radio galaxies, and LINERs.

In this partly ionized region, H^0, H, and free electrons coexist with neutral atoms of other elements, as well as with ions having an ionization potential similar to that of H. The dominant forms of O, S, and N in the partly ionized zone are O^0, S^+, and N^0, while smaller fractions of N^+ and O^+ are also present. Hot free electrons produced in this region by X-ray photoionization and by Auger processes can have a positive effect on the strengths of lines produced by collisional excitation. Important lines such as [O I] $\lambda 6300$, [S II] $\lambda\lambda 6716$, 6713, [N I] $\lambda 5199$, and [N II] $\lambda 6583$ are of this type. This extended zone of partly ionized H does not exist in H II regions photoionized by hot stars (e.g., Osterbrock 1974).

The critical densities for collisional de-excitation of [O I] $\lambda 6300$, [O III] $\lambda 5007$, [S II] $\lambda\lambda 6716$, 6731, [N I] $\lambda 5199$, and [N II] $\lambda 6583$ are respectively 2×10^6, 7×10^5, 2×10^3, 4×10^3, 2×10^3, and 9×10^4 cm^{-3}, using the atomic parameters collected by Mendoza (1983). Note the low values for [S II] and [N I]. Measured line ratios of [S II] $\lambda\lambda 6716$, 6731 show that in nearly all Seyfert 2 and narrow-line radio galaxies these lines are appreciably collisionally de-excited. The same must be true of [N I] $\lambda 5199$. Evidently [S II] $\lambda\lambda 6716$, 6731 are nevertheless strong, because nearly all S is S^+ and because of the large collisional-excitation cross sections for these lines. [N I] has a much smaller excitation cross section, and although it is no doubt strengthened in AGNs with respect to H II regions, it is still weak.

We can now understand the distribution of data points in Figures 1–6. The intensities of [O I] $\lambda 6300$, [S II] $\lambda\lambda 6716$, 6731, and [N II] $\lambda 6583$ are larger with respect to Hα in narrow-line AGNs than in H II region–like objects because collisional excitation of these lines is more important in objects with extended partly ionized zones. Since the ionization potential of O^0 matches the ionization potential of H very well, we should expect a large difference between the [O I] $\lambda 6300/H\alpha$ ratios of H II region–like objects and of narrow-line AGNs exactly as found in Figures 3 and 6. The effect is also important for [S II] $(\lambda 6716+\lambda 6731)/H\alpha$ as seen in Figures 2 and 5, but the fact that S^+ can also exist within the H^+ zones of H II regions and AGNs somewhat attenuates the difference between the two classes of objects.

The behavior of [N II] $\lambda 6583$ is more difficult to interpret. N^+, like other singly ionized elements with ionization potentials greater than 13.6 eV, is present in the outer partly ionized zone but is not the predominant stage. Hence it is expected to be strengthened, but not as greatly as [S II], in the absence of collisional de-excitation. Perhaps [N II] is strengthened as greatly as it is because it is not appreciably collisionally de-excited, as [S II] is. Simple one-density models do not show this effect and therefore suggest that AGNs may possibly have higher N abundances. More sophisticated pho-

toionization models incorporating physically plausible mixtures of electron densities must be explored before this interpretation can be regarded as proved.

Photoionization by high-energy photons and Auger processes are especially efficient in heating the gas in AGNs, which therefore must have a somewhat higher equilibrium temperature than the gas in H II region galaxies photoionized by stars. This effect may also explain in part why [N II] λ6583 is relatively strong in narrow-line AGNs than in H II region–like galaxies.

Finally, O^{++} is produced predominantly by UV photons ($h\nu > 35$ eV) well inside the partly ionized zone and close to the ionizing source. The effects of the most energetic X-ray photons are not very important in that region. However, the relatively larger numbers of photons that can ionize O^{+} to O^{++} in the power-law type spectra generally make [O III] $\lambda 5007/H\beta$ larger in the AGNs of our sample than in all but the highest excitation H II region–like objects. Contrary to early statements (Shuder and Osterbrock 1981), there are H II region galaxies with [O III] $\lambda 5007/H\beta > 3$, but they are relatively uncommon.

With this understanding of the distribution of data points in our diagrams, we are in a good position to define quantitative limits separating the H II region–like objects from the narrow-line AGNs. The positions of these boundaries that best divide the NELGs into H II region–like galaxies and narrow-line AGNs are shown as solid lines in Figure 1–6. The general shapes of these curves were based directly on the photoionization models of § III, which present the same kind of behavior. Of course the positions of these boundary curves are not perfectly determined. This is especially true of the extremities of the curves. Considering the uncertainties of the line intensity ratios and of the positions of the curves, the nature of any object within the "transition zones" within ±0.15 (horizontally) of these boundaries is very difficult to determine. Such galaxies may be either pure H II region–like objects or pure narrow-line AGNs that because of errors in the line ratios have been shifted toward the boundary. It is also quite possible that both types of excitation mechanism are present in the same galaxy (Binette 1985). Another possibility is that the ionization in the nuclei of these objects is caused by a central "power-law" source, while outside the nuclei ionization by hot stars is predominant. The ratios of line intensities measured through finite-size apertures are weighted averages of the line intensities produced by two different ionization processes. This blending of the emission lines of the nucleus with those of H II regions in the disk of a galaxy is especially serious for distant and therefore angularly small galaxies (Dressler, Thompson, and Shectman 1985).

In trying to decide whether an object is an H II region galaxy or a narrow-line AGN, more weight should be given to the diagram of [O III] $\lambda 5007/H\beta$ versus [O I] $\lambda 6300/H\alpha$ than to the other two diagrams, because, for the reasons stated above, the separation between the two classes of objects is much more distinct in the diagram involving the [O I] line.

A few objects in our sample fall in the domain of H II region–like galaxies in certain diagram(s), but in the region of AGNs in other diagram(s). An outstanding example is the object observed as the radio galaxy 3C 178 by Costero and Osterbrock (1977) on the basis of an identification believed valid at that time. It is plotted as a narrow-line radio galaxy in Figures 1–3, and as a half-filled circle in Figures 4–6. In the first three diagrams it is the one narrow-line radio galaxy that appears out of place. Its ratios are typical of an H II region galaxy. However, a more recent accurate radio position determined by Haschick *et al.* (1980) shows that the object Costero and Osterbrock (1977) observed is not the radio galaxy 3C 178. The object they observed is an H II region galaxy that is by no means exceptional, while 3C 178 is presumably a much fainter and still unidentified quasar. This is a striking confirmation of the classification scheme.

TABLE 5

CLASSIFICATION OF NARROW–EMISSION-LINE GALAXIES

Narrow-Line AGNs	H II Galaxies
M 81	NGC 4670
NGC 5005	Mrk 111
Mrk 266 NE	Mrk 111 comp
Mrk 833	Mrk 432 W
Mrk 938	Mrk 490 A + B
Mrk 945	Mrk 490 C
Mrk 1127	Mrk 540
Mrk 1133	Mrk 724
Mrk 1144	Mrk 1040 comp
I Zw 81	Mark 1149
	Mrk 1158
	Mrk 1178
	Mrk 1212
Uncertain	Mrk 1259
	Mrk 1308
NGC 6764	Mrk 1414
Mrk 185	Mrk 1459
Mrk 378	Akn 145
Mrk 739 W[a]	Akn 179
Akn 160	Akn 534
	Kaz 26
	Kaz 27
	UM 60
	UM 71
	UM 213

[a] Mrk 739 E is a Seyfert 1 galaxy.

Two Seyfert 2 galaxies are also interesting. Mrk 298 has a small [N II] $\lambda 6583/H\alpha$ which puts it into the H II region area at $\log$ [O III] $\lambda 5007/H\beta = 0.29$ in Figures 1 and 4. However, its relative intensities of [S II] ($\lambda 6716 + \lambda 6731$) and [O I] λ6300 are typical of narrow-line AGNs. The other exceptional Seyfert 2 is the very high-ionization galaxy Mrk 1388 (Osterbrock 1985), at $\log$ [O III] $\lambda 5007/H\beta = +1.03$, but with quite weak [S II].

Four objects in Keel's (1983) sample are not positively classified as narrow-line AGNs according to these diagrams. They are NGC 3627, NGC 2639, NGC 4102, and NGC 4569 (with $\log$ [O III] $\lambda 5007/H\beta = 0.69, -0.59, -0.42$, and -0.22, respectively). They are shown as LINERs in Figures 1–3 but as half-filled circles in Figures 4–6. The exceptional behavior of NGC 3627 is probably due to instrumental problems (Keel 1983). Keel notes that the Hβ flux of NGC 4102 is uncertain. The line ratios [O III] $\lambda 5007/H\beta$ of the other two objects were based on the assumption that $H\alpha/H\beta = 3.0$, since Hβ was not measured in these objects. These four points are thus all fairly uncertain.

Among the H II region–like objects, three objects deserve comment. They are also shown as half-filled circles in Figures 4–6. Mrk 213 is a starburst galaxy with line ratios log [O III] $\lambda 5007/H\beta = 0.51$ and log [N II] $\lambda 6584/H\alpha = -0.36$ (Balzano 1983). Its position among the narrow-line AGNs in Figure 4 is probably due to the large uncertainty of its line ratios. The position of the H II region in NGC 4395 is near the region occupied by Seyfert 2 nuclei (log [O III] $\lambda 5007/H\beta = 0.76$). This may be an indication that a nonthermal continuum (or shocks) also contributes to the ionization, since this H II region is only 5".1 from the center of the galaxy.

Finally, on the basis of the boundaries between H II region galaxies and AGNs as drawn in these diagrams, we can attempt to reclassify the galaxies previously published as NELGs. Their line ratios are taken from the data referenced in Table 1. Their new classifications are listed in Table 5. Five objects, as listed, are still uncertain, too close to the boundaries to be definitely called either H II region–like galaxies or AGNs.

V. SUMMARY

Large sets of internally consistent data on emission-line galaxies have been compiled from the literature. Whenever possible, a single dereddening procedure was applied to these data. The newly measured line ratios in the spectra of 50 additional emission-line galaxies were also included in the study and are presented in Tables 2–4. It was shown that the reddening-insensitive line ratios [O III] $\lambda 5007/H\beta$, [N II] $\lambda 6583/H\alpha$, [S III] $(\lambda 6716 + \lambda 6731)/H\alpha$, and [O I] $\lambda 6300/H\alpha$ are very useful in classifying emission-line galaxies into narrow-line active galaxies and H II region galaxies. The results of this classification along with the prediction of recent photoionization models by power-law spectra and by hot stars are presented in Figures 1–6. It was shown that the diagram of [O III] $\lambda 5007/H\beta$ versus [O I] $\lambda 6300/H\alpha$ is probably the best single tool presently available for discriminating between the two types of objects, in spite of the fact that very few measurements of [O I] $\lambda 6300$ have to date been published for H II region galaxies. It has also been shown that most of the so-called NELGs of Shuder and Osterbrock (1981) are either H II region galaxies or low-ionization narrow-line active galaxies (LINERs), as listed in Table 5.

We are very grateful to Drs. M. M. De Robertis and R. A. Shaw for numerous discussions and assistance in obtaining these data, and to the National Science Foundation for partial support of the research under grant AST 83-11585. S. V. would like to thank also the National Sciences and Engineering Research Council of Canada for financial support.

REFERENCES

Baldwin, J. A., Phillips, M. M., and Terlevich, R. 1981, *Pub. A.S.P.*, **93**, 5 (BPT).
Balzano, V. A. 1983, *Ap. J.*, **268**, 602.
Binette, L. 1985, *Astr. Ap.*, **143**, 334.
Brocklehurst, M. 1971, *M.N.R.A.S.*, **153**, 471.
Costero, R., and Osterbrock, D. E. 1977, *Ap. J.*, **211**, 675.
Davidson, K., and Netzer, H. 1979, *Rev. Mod. Phys.*, **51**, 715.
De Robertis, M. M., and Osterbrock, D. E. 1986, *Ap. J.*, **301**, 727.
Dinerstein, H., and Shields, G. A. 1986, *Ap. J.*, **311**, 45.
Dopita, M. A. 1976, *Ap. J.*, **209**, 395.
_____. 1977, *Ap. J. Suppl.*, **33**, 437.
Dressler, A., Thompson, I. B., and Shectman, S. A. 1985, *Ap. J.*, **288**, 481.
Evans, I. N., and Dopita, M. A. 1985, *Ap. J. Suppl.*, **58**, 125.
Ferland, G. J., and Netzer, H. 1983, *Ap. J.*, **264**, 105 (FN).
Ferland, G. J., and Osterbrock, D. E. 1986, *Ap. J.*, **300**, 658.
Filippenko, A. V., and Sargent, W. L. W. 1985, *Ap. J. Suppl.*, **57**, 503.
Fosbury, R. A. E., Mebold, U., Goss, W. M., and Dopita, M. A. 1978, *M.N.R.A.S.*, **183**, 549.
French, H. B. 1980, *Ap. J.*, **240**, 41.
Gaskell, C. M. 1984, *Ap. J. (Letters)*, **24**, 43.
Gaskell, C. M., and Ferland, G. J. 1984, *Pub. A.S.P.*, **96**, 393.
Goodrich, R. W., and Keel, W. C. 1986, *Ap. J.*, **305**, 148.
Goodrich, R. W., and Osterbrock, D. C. 1983, *Ap. J.*, **269**, 416.
Halpern, J. P., and Steiner, J. E. 1983, *Ap. J. (Letters)*, **269**, 637.
Haschick, A. D., Crane, P. C., Greenfield, P. E., Burke, B. F., and Baan, W. A. 1980, *Ap. J.*, **239**, 774.
Heckman, T. M. 1980, *Astr. Ap.*, **87**, 142.
Huchra, J. P. 1977, *Ap. J. Suppl.*, **35**, 171.
Hummer, D. G., and Mihalas, D. M. 1970, *M.N.R.A.S.*, **147**, 339.
Keel, W. C. 1983, *Ap. J.*, **269**, 466.
Keel, W. C., and Miller, J. S. 1983, *Ap. J. (Letters)*, **266**, L89.
Khachikian, E. Y., and Weedman, D. W. 1974, *Ap. J.*, **192**, 581.
Koski, A. T. 1978, *Ap. J.*, **223**, 56.
Koski, A. T., and Osterbrock, D. E. 1976, *Ap. J. (Letters)*, **203**, L49.
Kwan, J. and Krolik, J. H. 1981, *Ap. J.*, **250**, 478.
Lauer, T. R., Miller, J. S., Osborne, C. S., Robinson, L. B., and Stover, R. J. 1984, Proc. SPIE, **445**, 132.
Markarian, B. G., Lipowitsky, V. A., and Stepanian, D. A. 1983, *Astrofizika*, **19**, 29 (English transl. in *Astrophysics*, **19**, 14 [1983]).
Mathis, J. S. 1970, *Ap. J.*, **159**, 263.
McCall, M. L. 1982, Ph.D. thesis, University of Texas at Austin (Astronomy Department Publication, No. 20).
McCall, M. L., Rybski, P. M., and Shields, G. A. 1985, *Ap. J. Suppl.*, **57**, 1.
Mendoza, C. 1983, in *IAU Symposium 103, Planetary Nebulae*, ed. D. R. Flower (Dordrecht: Reidel), p. 143.
Meurs, E. J. A. 1982, Ph.D. thesis, University of Leiden.
Meurs, E. J. A., and Wilson, A. S. 1984, *Astr. Ap.*, **136**, 206.
Miller, J. S., and Mathews, W. G. 1972, *Ap. J.*, **172**, 593.
Netzer, H. 1980, *Ap. J.*, **236**, 406.
Osterbrock. D. E. 1974, *Astrophysics of Gaseous Nebulae* (San Francisco: Freeman).
_____. 1984, *Quart. J.R.A.S.*, **18**, 1.
_____. 1985, *Pub. A.S.P.*, **97**, 25.
Osterbrock, D. E., and Dahari, O. 1983, *Ap. J.*, **273**, 478.
Osterbrock, D. E., and De Robertis, M. M. 1985, *Pub. A.S.P.*, **97**, 1129.
Péquignot, D. 1984, *Astr. Ap.*, **131**, 159.
Raymond, J. C. 1979, *Ap. J. Suppl.*, **39**, 1.
Rose, J. A., and Tripicco, M. J. 1984, *Ap. J.*, **285**, 55.
Schild, R. E. 1977, *A.J.*, **82**, 337.
Searle, L. 1971, *Ap. J.*, **168**, 327.
Shields, G. A., and Oke, J. B. 1975, *Ap. J.*, **197**, 5.
Shuder, J. M., and Osterbrock, D. E. 1981, *Ap. J.*, **250**, 55.
Shull, J. M., and McKee, C. J. 1979, *Ap. J.*, **227**, 131.
Stasinska, G. 1980, *Astr. Ap.*, **84**, 320.
_____. 1982, *Astr. Ap. Suppl.*, **48**, 299.
_____. 1984*a*, *Astr. Ap. Suppl.*, **55**, 15.
_____. 1984*b*, *Astr. Ap.*, **135**, 341.
Stauffer, J. R. 1982, *Ap. J.*, **262**, 66.
Wampler, E. J. 1971, *Ap. J.*, **164**, 1.
Weedman, D. W., Feldman, F. R., Balzano, V. A., Ramsey, L. W., Sramek, R. A., and Wu, C.-C. 1981, *Ap. J.*, **248**, 105.
Weisheit, J. C., Shields, G. A., and Tarter, C. B. 1981, *Ap. J.*, **245**, 406.

DONALD E. OSTERBROCK and SYLVAIN VEILLEUX: Lick Observatory and Board of Studies in Astronomy and Astrophysics, University of California, Santa Cruz, CA 95064.